Toward recycling unsortable post-consumer WEEE stream: Characterization and impact of electron beam irradiation on mechanical properties

Imane Belyamani, Joachim Maris, Sylvie Bourdon, Jean-Michel Brossard, Laurent Cauret, Laurent Fontaine, V. Montembault

Amount of words? 7865 words excluding the title page

Toward recycling ″unsortable″ post-consumer WEEE stream: Characterization and impact of electron beam irradiation on mechanical properties

Imane Belyamani[a*], Joachim Maris[b,c], Sylvie Bourdon[b], Jean-Michel Brossard[b], Laurent Cauret[a], Laurent Fontaine[c], Véronique Montembault[c*]

[a] *Institut Supérieur de Plasturgie d'Alençon (ISPA), Pôle Universitaire de Montfoulon, BP 823, 61041 Alençon Cedex (France)*

[b] *Veolia Recherche et Innovation, Zone portuaire de Limay, 291 Avenue Dreyfous-Ducas, 78520 Limay (France)*

[c] *Institut des Molécules et Matériaux du Mans (IMMM) - UMR 6283 CNRS, Le Mans Université, Avenue Olivier Messiaen, 72085 Le Mans Cedex 9 (France)*

*Corresponding authors:
E-mail : veronique.montembault@univ-lemans.fr,
imane.belyamani@zu.ac.ae

Abstract

The work reported here is the first study aimed at providing a full screening of a real unsortable non-recycled post-consumer WEEE stream free of brominated flame retarded plastics, separated using on-line X-ray detection, toward its recycling. In the existing sorting lines, up to 40% of plastics from waste electrical and electronic equipment (WEEE) stream can be rejected, herein named unsortable plastics, To have the most representative homogeneous sample for physico-chemical characterizations, a sampling method was developed to overcome the heterogeneity of the investigated 500 kg batch. The batch screening on both representative samples (~500 µm size) and 100 plastic fractions (~20 mm size), by means of routine techniques used in the plastic industry, has allowed to quantify reliably the main polymers included in the studied batch; ~50 % styrene-based polymers, ~15 % polypropylene (PP), ~15 % polycarbonate (PC), ~1-4 % polyamide (PA), polyethylene (PE), polyvinyl chloride (PVC), poly(ethylene terephthalate) (PET), poly(methyl methacrylate) (PMMA) and ~8 % of multi-layer plastics, paints and thermosets. The identification of the ~8.0% inorganic phase by X-ray fluorescence spectrometry revealed the presence of several additives/charges commonly incorporated in plastic materials, such as calcium carbonate and talc. The studied batch was then subjected to electron beam irradiation at 50 and 200 kGy doses, as a means of compatibilization between the batch components. The mechanical properties and thermal behavior of irradiated samples pointed out the crucial role of the residual free radical scavenger agents present in post-consumer WEEE streams, leading to significantly different properties compared to those of irradiated virgin polymer blends highlighted in the literature.

Keywords:

Unsortable plastics, Post-consumer WEEE, Electron beam irradiation, Sampling method, Plastics recycling, Mechanical properties

1. Introduction

Waste electrical and electronic equipment (WEEE) is the fastest growing source of waste, potentially rising 4% per year (Sahajwalla and Gaikwad, 2018). This increasing waste stream has led to the publication of directive 2012/19/EU by the European Commission, targeting a WEEE recycling rate between 55% and 80% (2012/19/EU, 2012). WEEE is a complex stream consisting of a mixture of metals (Kyere et al., 2018), ceramics, glass and plastics. The proportion of the latter, depending on the six WEEE categories defined in directive 2012/19/EC (2012/19/EU, 2012), is ranging between 10 wt.% and 33 wt.% (Gramatyka et al., 2007; Kang and Schoenung, 2005; Parajuly and Wenzel, 2017; Vazquez and Barbosa, 2016; Wang and Xu, 2014; Widmer et al., 2005). Therefore, to achieve the objectives set out in directive 2012/19/EC, WEEE plastic recycling is imperative. Furthermore, plastic waste management has become an ecological issue given the need to limit the impact of plastics on our environment (Dolores et al., 2020; Hamaide et al., 2014; Ismail and Hanafiah, 2019; Milad et al., 2020); From an economical point of view, studies on the plastic composition in WEEE reported in the literature highlighted the presence of different types of polymers, the amount of which varies with the source (Alwaeli, 2011; Bovea et *al.*, 2016; Chancerel and Rotter, 2009; Dimitrakakis *et al.*, 2009; Maris *et al.*, 2015; Martinho *et al.*, 2012; Stenvall *et al.*, 2013; Taurino *et al.*, 2010). Considering the economic effectiveness of the waste utilized as substitutes for primary materials, as discussed by Alwaeli (2011), only the most representative polymers of the stream, that can be technically sorted and valorized according to the regulatory, are separated individually for further mechanical recycling operations. The plastic composition of WEEE issued from small electrical and electronic equipment (EEE) recycling units in Europe consists mainly of acrylonitrile-butadiene-styrene copolymer (ABS), polypropylene (PP), polystyrene (PS), and high-impact polystyrene (HIPS)

(Dimitrakakis *et al.*, 2009; Maris *et al.*, 2015; Martinho *et al.*, 2012). Up to now, the complexity and financial cost of plastic sorting makes difficult to consider the separation of the plastics from each other to facilitate recycling of a single type of polymer.

In the past decade, near infrared spectroscopy (NIR) has been integrated in the recycling process of WEEE (Menad, 2016), and allows to separate automatically on line the ABS, PP and PS from waste white plastics with a high accuracy up to 99% (Li *et al.*, 2019). This technique can potentially detect other plastics. However, it is not always relevant to the amount of each plastic and the economic issues related to sorting schemes. As a result, about 40% of WEEE plastics are rejected from the sorting line, herein named unsortable (Fig. 1), because i) they do not comply with sorted resins, ii) they contain dark pigments, named black plastics (Maris et al., 2015), which are not recognized by the classical NIR equipment or iii) because they contain brominated flame retardants (BFR), estimated to be ~25% of WEEE plastics (Hennebert, 2017). Using on-line X-ray detection, BFR-containing plastics are separated as specified in the directive 2019/1021/EU (2019/1021/EU, 2019). Indeed, the recovery of brominated flame retarded plastics has been restricted to treatments that destroy or irreversibly transform the substances, as stated in 2012/19/EC directive and Stockholm convention (2012/19/EU, 2012; Stockholm Convention, 2017).

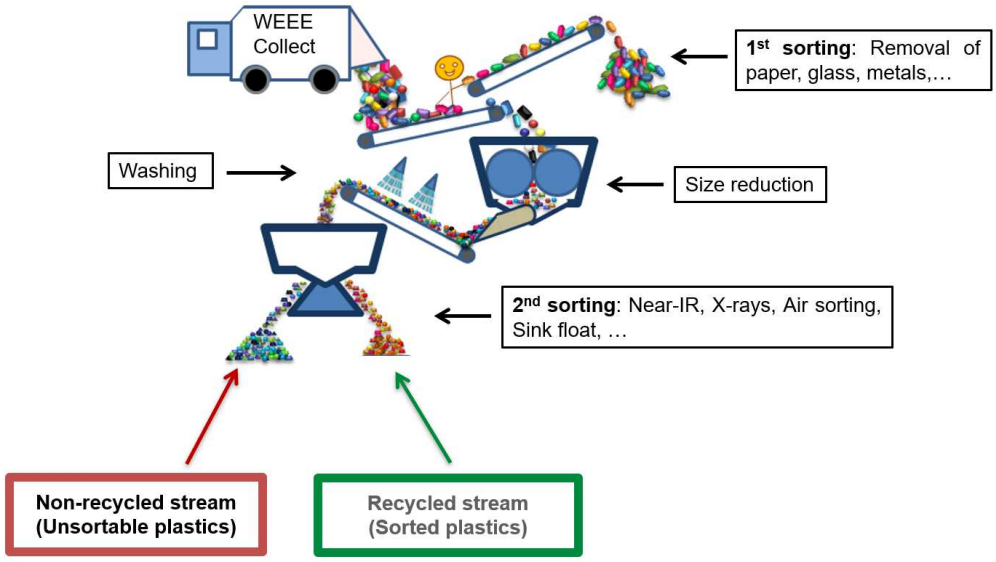

Fig. 1. General sorting steps for post-consumer WEEE plastic waste

Based on this observation, Tostar *et al.* (2016) have studied recycling of a polymer blend based on 80 wt.% styrene-based polymers and 10 wt.% PP from WEEE, by adding a compatibilizer or by gamma irradiation. The irradiation of polymeric materials with ionizing radiation appears to be a promising tool to chemically modify polymers as it leads to the formation of free radicals along the backbone even on low reactive polymers, such as polyolefins (Burillo *et al.*, 2002; Chmielewski *et al.*, 2005). The compatibilization is ensured by (i) direct crosslinking between macroradicals of two polymers to form new covalent bonds (Gu *et al.*, 2014; Li *et al.*, 2009) or (ii) indirect crosslinking via a coupling agent binding two polymers (Lambla and Seadan, 1993, 1992; Xanthos and Dagli, 1991). The resulting copolymers act as a compatibilizing agent which concurrently lower the interfacial tension at phase boundaries and enhance their adhesion, leading to an improvement of the mechanical properties (Maris *et al.*, 2018; Utracki, 2002). For example, the mechanical properties of a blend of seven virgin polymers frequently found in plastic solid waste: low-density polyethylene (LDPE), high-density polyethylene (HDPE), poly(vinyl chloride) (PVC), PS, HIPS, PP, and poly(ethylene terephthalate) (PET) were improved through the addition of

peroxides (Vivier and Xanthos, 1994). Similarly, Said *et al.* (2013) have reported an enhancement of the tensile properties of different PET/LDPE mixture compositions subjected to gamma irradiation at 25 and 50 kGy doses. Blends of waste polyethylene/LDPE 70/30, exposed to electron beam (EB) irradiation at doses up to 300 kGy, showed higher ductility, toughness, and resistance to oxidative degradation. These irradiated blend materials were successfully blow molded to make bottles (Satapathy *et al.*, 2006).

Apart from Taurino *et al.* (2010) investigations on characterization of two sorted black/grey plastic waste categories (i.e. personal computers and televisions), the work reported in this article is the first study aimed to analyze and provide a full screening of a real unsortable non-recycled post-consumer WEEE stream.

In this contribution, for the first time the composition of unsortable post-consumer WEEE plastics stream free of BFR, sorted using on-line X-ray technique as specified in the directive 2019/1021/EU, was investigated. The studied 500 Kg batch was collected in France from the following streams: cooling appliances, household electrical equipment, and information technology (IT), such as computers, printers and phones. The polymer and additives/charges composition of unsortable plastics has been determined using Fourier-transform infrared (FTIR) spectroscopy, X-ray fluorescence spectrometry, differential scanning calorimetry (DSC), and thermogravimetric analysis (TGA).

Burillo *et al.*, 2002; Fel *et al.*, 2016; Lambla and Seadan, 1993; Numata and Fujii, 1995; Said *et al.*, 2013; Satapathy *et al.*, 2006; Tostar *et al.*, 2016; Vivier and Xanthos, 1994 have reported the impact of irradiation process on polymer blend. In contrast to these cited studies where polymer blend recycling was simulated on the basis of virgin polymers or unsorted plastics, the present work provides a comprehensive investigation on EB-irradiated unsortable post-consumer WEEE batch prior to melt-process. EB irradiation has the advantage of being a

clean and continuous process that is already commercially well-established (Drobny, 2010). Thus, the impact of EB irradiation doses (50 and 200 kGy) on thermal behavior and mechanical properties of the studied batch was investigated.

2. Experimental Section

2.1. Materials

A 500 kg big bag of unsortable post-consumer WEEE, collected in April 2015, was supplied by Veolia (France). Liquid nitrogen used to grind the sample was provided by Air Liquide (France).

2.2. Sampling procedure

The sampling procedure was carried out on a 500 kg batch with heterogenous fraction sizes (<70 mm) from unsortable post-consumer WEEE stream. In order to have the most representative homogeneous sample for physico-chemical characterizations, a sampling method is necessary to overcome the heterogeneous constitution and size distribution of the tested batch. For this study, we developed a sampling method (see Fig. 2) based on Gy (1998) work and the XP CEN/TS 17188 standard (Afnor, 2018), and adapted from our research team previous work (Epsztein *et al.*, 2014).

2.3. Melt Processing and Characterization Methods

2.3.1. *Twin-screw extrusion*

Extrusion experiments were carried out using a co-rotating twin-screw extruder Coperion ZSK18 (L/D = 40). The barrel temperature along the interpenetrate screws (feeding to die) was set at 190, 190, 200, 200, 200, 200, 200, 210, 210 and 210 °C with a screw speed of 250 rpm. The obtained extrudates were pelletized after cooling.

2.3.2. *Injection molding*

Dog-bone specimens 1A ISO 527 type and impact bars (80 x 10 x 4 mm^3) were injection molded using a Krauss Maffei EX80-380 injection molding extruder. The detailed processing parameters are summarized in Table S1.

2.3.3. *Fourier-transform infrared spectroscopy (FTIR)*

Infrared spectra were collected in the wavenumber range 400–4000 cm^{-1} using a Fourier transform spectrometer Nicolet 380 DTGS in transmission mode for micro-ground samples, and ATR (attenuated total reflection) mode for bulk samples. Spectra were recorded at a resolution of 2 cm^{-1} and 128 scans. The pellet samples for the transmission mode were prepared by grinding micro-ground sample (~500 µm) and KBr powder with a ratio of 10:100, and then pressing the mixture into pellets.

2.3.4. Differential scanning calorimetry (DSC)

Differential scanning calorimeter analysis was carried out on ~7 mg representative sample using a Q100 TA Instrument under standardized conditions ISO 11357. Samples were equilibrated at -50 °C, ramped at a heating rate of 10 °C/min to 280 °C, cooled down to -50 °C and re-heated to 280 °C at the same heating rate, under nitrogen atmosphere. The reported data represent the cooling and the second heating cycles for three replicates.

2.3.5. *Thermogravimetric analysis (TGA)*

Thermal behavior of the studied samples was investigated on ~13 mg representative sample, following the ISO 11358 standard, using a TGA1 analyzer from Mettler Toledo. Tests were performed from 50 to 900 °C under nitrogen atmosphere (flow of 45 mL/min) at a heating rate of 10 °C/min. After 1 min isothermal at 900 °C under nitrogen, the atmosphere was switched to dry air and kept for 10 min at 900 °C. The repeatability of the measurement was evaluated on the basis of three replicates.

2.3.6. Energy dispersive X-ray fluorescence (XRF)

178 The XRF data were collected with a wavelength dispersive X-ray spectrometer PW2404-
179 DY 750 Philips equipped with a rhodium X-ray tube anode and operated at 2.4 kW power for
180 all measurements using vacuum conditions. To investigate possible interferences, different
181 scans were performed using a 27 mm collimator and five crystals: LiF 200, LiF 220, Ge, InSb
182 and PX1. The XRF test specimens were obtained by compression molding the representative
183 sample powder at 160 °C, under manual pressure of ~15 bars. The reported values represent
184 the average of three replicates.

185 ***2.3.7. Electron beam irradiation***

186 EB irradiation was performed on extruded pellets and micro-ground samples by Ionisos SA
187 (France) using a commercial EB accelerator source of ^{60}Co, under room temperature and air
188 atmosphere. The tested irradiation doses (50 and 200 kGy) were controlled by varying the
189 automatic conveyor speeds. Acceleration energy was set at 0.7 ± 0.2 MeV.

190 ***2.3.8. Tensile strength***

191 Tensile strength tests were carried out on injection molded dog-bone specimens 1A ISO
192 527 type, according to ISO 527 standard, using MTS Criterion® 43 test machine. Samples
193 were equilibrated at ~23 °C and ~50% relative humidity (RH) for at least 48h before testing
194 them under the same environmental conditions. The reported values represent the average of
195 ten replicates for tensile stress and tensile stains, and of five replicates for Young moduli.

196 **2.3.9. *Impact toughness***

197 Horizontal Charpy impact tests were carried out as per ISO 179 standard on unnotched
198 injection molded sample bars, using ZWICK 5102.202 impact pendulum device. Samples
199 were equilibrated at ~23 °C and ~50% RH for at least 48h before testing them under the same
200 environmental conditions. The reported impact toughness values were calculated for ten
201 replicates.

202 **3. Results and discussion**

3.1. Composition of the studied unsortable WEEE batch

Being aware of the composition and fraction size distribution (<70 mm) heterogeneity of the studied batch, a sampling method turned out to be necessary to obtain the most representative sample from the supplied big bag. Thus, we adapted a sampling method based on our research team previous work (Epsztein *et al.*, 2014), as detailed in Fig. 2.

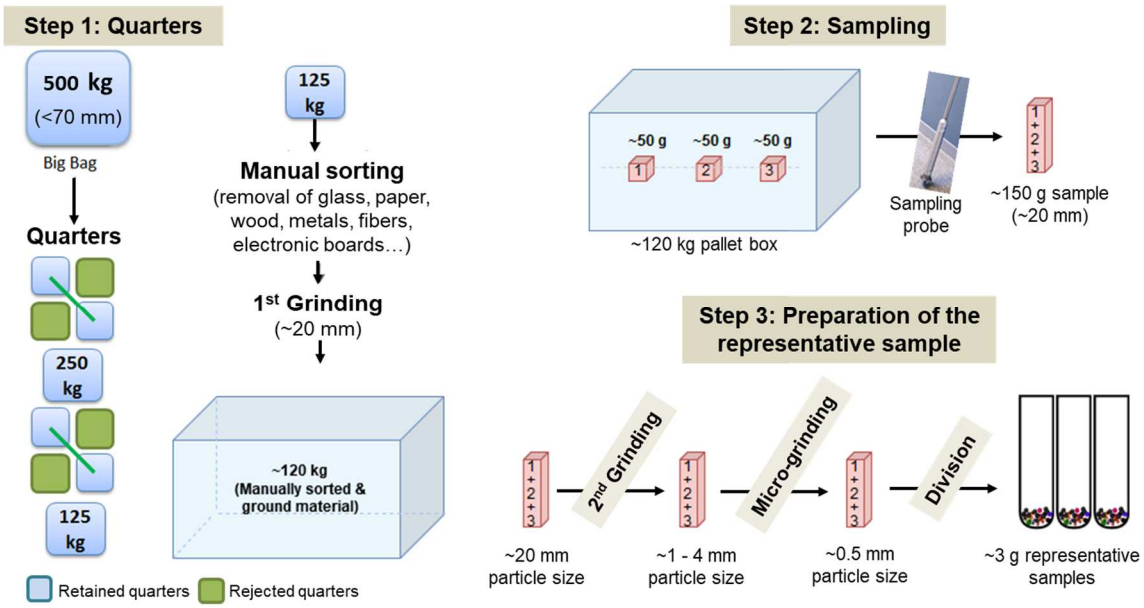

Fig.2. Sampling method used in the present study

The 500 kg batch was first spread out and divided into four quarters twice, and at each time, only two quarters were retained to finally obtain a 125 kg batch sample. After a manual sorting, aimed at removing residual metals, glass, paper…etc, the sample batch was ground to a particle size of ~20 mm, and three ~50 g samples were collected from the pallet box central horizontal axis using a sampling probe. The three collected samples were mixed, ground to a particle size of 2-4 mm, then to 500 µm. Finally, the ~150 g sample was divided using a rotating divider to obtain homogeneous representative sample fractions, of approximately 3 g, used for physico-chemical analysis.

3.1.1. Analysis of bulk samples

In order to quickly estimate the composition of the studied unsortable batch, 100 ground samples of ~20 mm size (Fig. 3a) were collected arbitrary from the ~120 kg pallet box (Fig. 2) and characterized by attenuated total reflection Fourier-transform infrared spectroscopy (ATR-FTIR). The polymer nature corresponding to each plastic fraction was identified by comparing the recorded ATR-FTIR spectra to that of the Omnic software database. Fig. 3b depicts the sum of assigned spectral polymers gathered from the 100 analyzed samples.

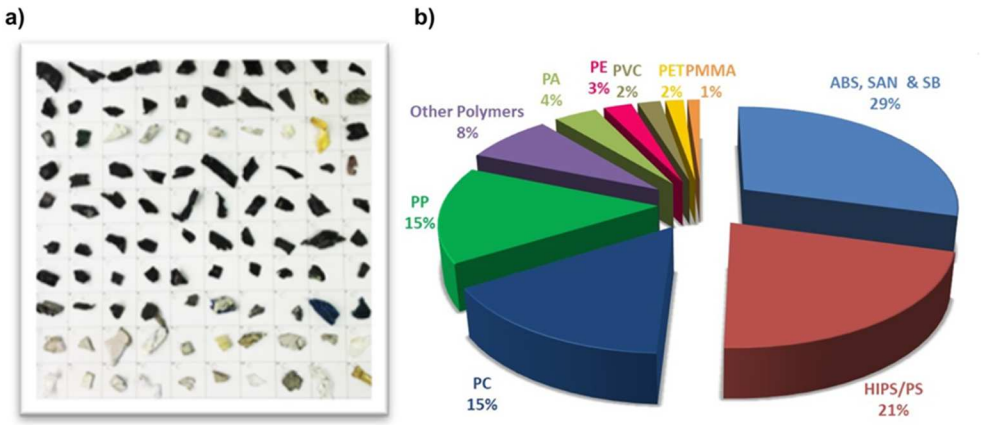

Fig. 3. a) 100 ground samples of ~20 mm size used to estimate b) the polymer composition, in %, of the studied unsortable batch using ATR-FTIR analysis.

The composition heterogeneity of the batch under investigation is clearly seen in Fig. 3. The collected sample is mainly constituted of styrene-based polymers (~50 %) such as acrylonitrile-butadiene-styrene (ABS), polystyrene (PS), high impact polystyrene (HIPS), poly(styrene-*co*-acrylonitrile) (SAN) and poly(styrene-*co*-butadiene) (SB). Polypropylene (PP) and polycarbonate (PC) represent about 15 % each. Polyamide (PA), polyethylene (PE), polyvinyl chloride (PVC), poly(ethylene terephthalate) (PET) and poly(methyl methacrylate) (PMMA) are present in a very low quantity (i.e. 1-4 %). It is worth noting that the ~8 % of "other polymers" include unidentified polymers such as multi-layer plastics, paints and thermosets. This preliminary polymer identification (Fig. 3) allows to determine qualitatively the polymer composition in the batch. Although this identification cannot be considered as

representative of the batch, the obtained results agree well with the data reported by Maris *et al.* (2015). Similarly, other studies carried out in Germany (Dimitrakakis *et al.*, 2009), and Portugal (Martinho *et al.*, 2012) on post-consumer plastic waste batches derived from small EEE showed that ABS, PS/HIPS (~50-56 wt.%) and PP (~25-30 wt.%) account for at least 70 wt.% of the total plastic weight, and that the weight percent of each polymer depends on the equipment type and WEEE categories (e.g. small household appliances, IT devices…).

3.1.2. Analysis of the batch representative sample

Likewise, the representative sample was characterized using FTIR, in the transmission mode, differential scanning calorimetry (DSC), thermogravimetric analysis (TGA) and energy dispersive X-ray fluorescence (XRF) to identify more reliably and quantitatively the composition of the studied batch before its melt processing and for further mechanical characterization. Through the different cited physico-chemical analysis, the following polymers, additives, charges and fillers were identified.

3.1.2.1. Styrene-based polymers

Table 1 presents the absorption bands observed on the FTIR transmission spectral signature (Fig. S1) and their assignment for the studied batch representative sample. It is clearly seen that the main screened constituents are styrene-based polymers. Indeed, the strong out-of-plane C-H bending bands at 697 and 757 cm^{-1}, and the aromatic C-C stretching bands at 1452, 1493 and 1601 cm^{-1} are characteristic of the aromatic substitution pattern. Additionally, the two (out of four) aromatic combination bands in mono-substituted benzene (1879 and 1941 cm^{-1}), usually observed for PS (Liang and Krimm, 1958; Munteanu and Vasile, 2005), confirm the presence of styrene pattern. The other two aromatic combination

262 bands (1745 et 1800 cm^{-1}) might be hidden due to the band overlapping as a consequence of

263 the complex composition of the studied batch.

264 **Table 1.** Observed FTIR absorption bands and their assignment for the representative sample
265 of the studied unsortable WEEE batch.

Wavenumber (cm^{-1})	Intensity	Assignments	Polymer type
697	vs	δ C-H aromatic	Styrene-based polymers
757	m		
1452	m	ν C-C aromatic	Styrene-based polymers
1493	w		
1601	w		
1879	vw	Aromatic combination bands in mono-substituted rings	PS
1941	vw		
2236	vw	ν C≡N	ABS, SAN
3025	w	ν C-H aromatic	Styrene-based polymers
3059	vw		
1640	w	ν C=C of 1,2-vinyl butadiene	ABS, HIPS, SB
909	w	δ CH_2 1,2-butadiene	
964	w	δ CH_2 *trans*-1,4-butadiene isomer	
1163	m	ν C-O & ν C-C aromatic	PC
1193	m	ν C-O & ν C-C aromatic	
1229	m	ν C-O	
1772	w	ν C=O	
1731	w	ν C=O	PET or PMMA
1376	w	δ CH_3	PP
2849	w	ν CH_2 polymer chains	PE
2917	m		
3298	vw	ν NH or ν OH	PA or degraded ABS respectively

266 vs: very strong; m: medium; w: weak; vw: very weak; ν: stretching vibrations; δ: bending vibrations

267

268 On the other hand, the absorption peaks of butadiene pattern recorded at 967 and 909 cm^{-1}

269 are representative of ABS, SB and/or HIPS; these polymers are mainly characterized by C–H

deformation in *trans*-1,4-butadiene isomer and in 1,2-butadiene units at 965 and 910 cm^{-1} respectively. The other butadiene characteristic band (i.e. 729 cm^{-1} for δCH_2 in *cis*-1,4-butadiene) (Lacoste *et al.*, 1996; Silas *et al.*, 1959) could not be detected. Nevertheless, the peak at 1640 cm^{-1} reflects the stretching vibrations of the C=C interaction in the 1,2-butadiene group (Munteanu and Vasile, 2005). Adding to that, the stretching vibrations of the nitrile group (C≡N), typical for ABS and SAN, was observed at 2236 cm^{-1}.

The presence of styrene-based polymers in the studied batch is also supported by DSC (Fig. 4a). As it is clearly seen in Fig. 4a, a glass transition temperature (T_g) around 99°C, distinctive of ABS, PS, HIPS and SAN, was identified.

3.1.2.2. Polyolefins

The DSC thermograms (Fig. 4a) depict two distinctive endothermic peaks at ~129-133°C and ~162-165 °C, typical of PE and PP melting temperatures (T_m *PE* and T_m *PP*), respectively. Besides, the cooling exotherms in Fig. S2 display two single crystallization peaks at temperatures corresponding to PP (*Tc* = ~120-121 °C) and PE (*Tc* = ~144-146 °C). Moreover, compared to the PP crystals melting enthalpy (~5.9-8.3 J/g), that of PE (~0.3-2.7 J/g) indicates a very low weight concentration of PE in the studied batch, which perfectly matches the FTIR data for bulk samples (Fig. 3b).

Interestingly, a higher temperature melting peak next to the main PP endothermic peak was observed at ~175 °C for two replicates (Fig. 4a). It is not clear whether this extra melting peak is a consequence of different PP lamellar arrangements that may result from polymer oxidation phenomenon, or simply the presence of α-phase isotactic PP crystals (Huy *et al.*, 2004) subsequent to different crystallization conditions that may have occurred during the manufacture processes.

3.1.2.3. Other polymers

Polyamides. The maximum absorption peak at ~3298 cm^{-1} (Table 1 and Fig. S1) could be assigned to stretching vibrations of NH bond, characteristic of polyamides. However, it has been shown that the degradation of ABS can lead to the OH moiety formation with a vibration band at ~3400 cm^{-1} (Li *et al.*, 2017). Furthermore, the large melting peak at ~220°C (Fig. 4a) and the crystallization one at ~190°C (Fig. S2) can be attributed to PA6, PA610 and/or PA612.

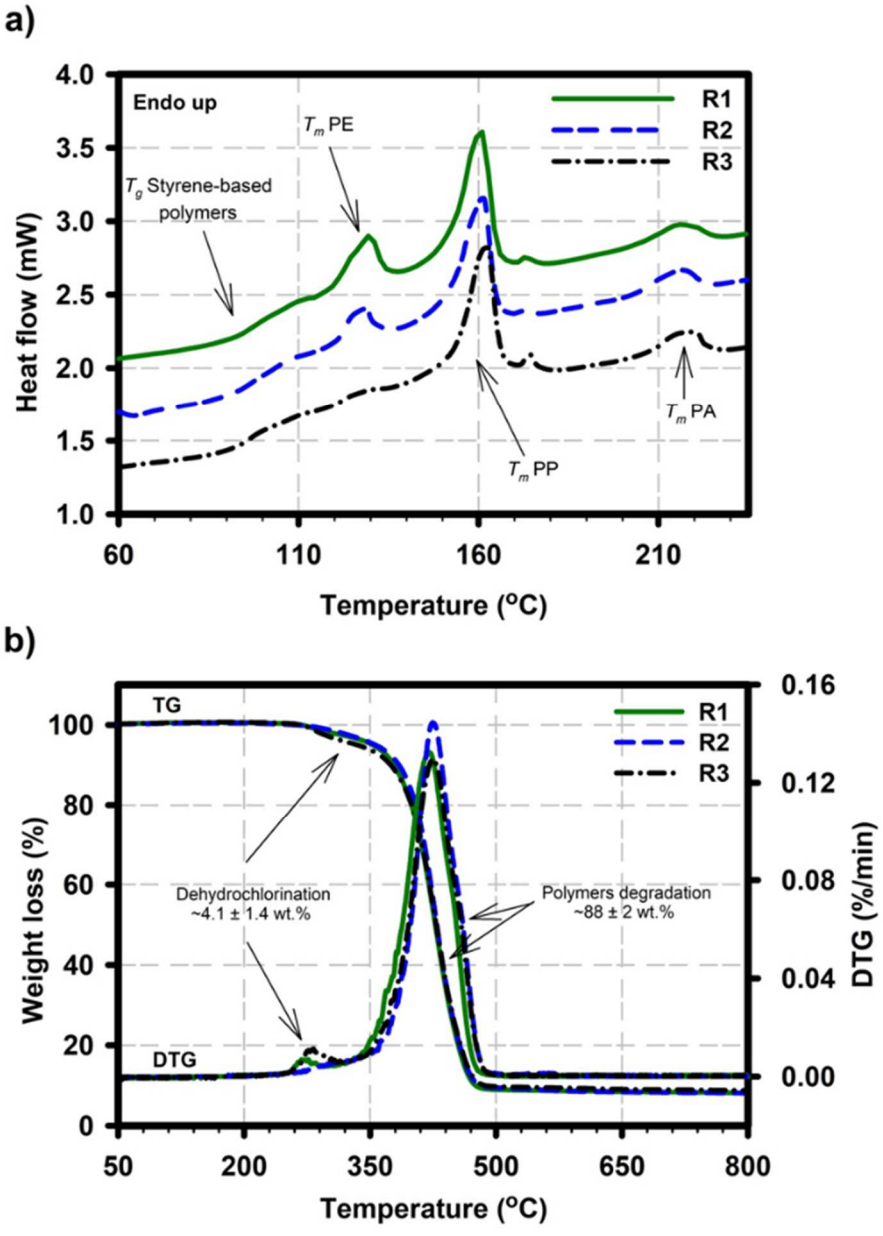

Fig. 4. a) 2nd heating DSC thermograms, and b) TG and DTG curves for three replicates (R1, R2, R3) of unsortable WEEE representative sample.

PC, PMMA, PET. The very low concentration of PMMA and PET in the studied batch (Fig. 3b) as well as the hiddenness of the PC T_g, covering the 145-150°C range, by other polymers thermal events (Fig. 4a and Fig. S2) make their detection by DSC impossible. Nonetheless, Fig. S1 and Table 1 exhibit several absorption peaks that may be associated with PC, PMMA or PET. Bands at 1772 cm^{-1}, assigned to stretching vibrations of C=O bond, and the absorption peaks between 1128 and 1235 cm^{-1} (Fig. S1), corresponding to stretching vibrations of C-O bond, involve the presence of PC (Ghorbel *et al.*, 2014). The band at 1731 cm^{-1} can also be attributed to stretching vibrations of C=O interactions of the ester function in PET or PMMA (Ghorbel *et al.*, 2014; Zhu and Kelley, 2005).

Although the mentioned absorption peaks emphasize the presence of PC, PMMA and PET, the same functional groups can also be ascribed to the degradation of styrenic polymers, either via thermo- (Karahaliou and Tarantili, 2009; Vilaplana *et al.*, 2006) or photo-oxidation (Gardette *et al.*, 1995) mechanisms.

PVC. The identification of PVC in the studied batch was achieved on the basis of TGA analysis. The first degradation observed in thermogravimetry (TG) and derivative thermogravimetry (DTG) curves at about 285°C (Fig. 4b) could be attributed to the presence of PVC and allows the estimation of ~4.1 ±1.4 wt. % of PVC in the sample. Indeed, it has been demonstrated that the degradation of PVC occurs in two stages (McNeill et al., 1995): i) the first one (250-360°C) corresponds to the dehydrochlorination and accounts for ~50 wt.% of the weight loss, and ii) the second one (360-500°C) is related to the polymer chains degradation. The latter accounts for ~25 wt.% weight loss. PVC content in the representative sample determined from TGA is twice as high as estimated by the ATR-FTIR analysis on the

100 plastic fractions (Fig. 3b). On the other hand, ~1.9 ± 0.4 wt.% of chlorine (Cl), coming mainly from PVC, was obtained from XRF analysis (Table 2). The over-estimated PVC concentration by TGA may be due to potential interactions between degradation products of the batch components that could enhance the dehydrochlorination rate of PVC, particularly in the presence of ABS and/or PET (Czégény et al., 2012).

3.1.2.4. Additives, charges and fillers

The complexity of the studied batch comes not only from the different types of polymers, as described above, but also from the numerous inorganic/organic additives commonly incorporated in plastic materials to improve their properties either mechanical, physico-chemical, thermal, rheological or even esthetic. TGA analysis (Fig. 4b) showed approximately 8.0 ± 0.3% under nitrogen residue, confirming the presence of an inorganic phase. XRF analysis of the studied batch has allowed a reliable screening of its elemental composition (Table 2). The validity of the sampling method is demonstrated by the low standard deviation of the replicates. Several additive systems were identified as a result of the elements examination.

Magnesium (Mg), aluminum (Al) and silicon (Si) are commonly used in the composition of mineral fillers, usually in the form of silicates such as talc (hydrated magnesium silicate, $Mg_3Si_4O_{10}(OH)_2$) or kaolin (hydrated aluminum silicate, $Al_2Si_2O_5(OH)_4$). Mg and Al elements can also be issued from the presence of hydrotalcite compounds ($Mg_6Al_2CO_3(OH)_{16}$, $4(H_2O)$), used as a heat co-stabilizer for PVC (Bao *et al.*, 2008). Calcium carbonate ($CaCO_3$) is the main Ca-based molecule frequently used in plastic industry with the purpose to decrease the final cost of the material and increase its mechanical properties. Nonetheless, calcium

oxide (CaO) in combination with silicon dioxide (SiO_2) and aluminum oxide (Al_2O_3), originated from fiberglass (Maris *et al.*, 2015), should not be ignored.

Table 2. Weight % of the different elements detected in the unsortable WEEE representative sample as determined by XRF.

Elements	Concentration (wt. %)		Elements	Concentration (wt. %)	
	Average	Error*		Average	Error*
H	7.917	0.050	Ba	0.143	0.042
C	82.366	0.665	S	0.112	0.015
N	1.865	0.021	Fe	0.145	0.012
O	2.175	0.192	Ni	0.011	0.001
Ca	0.859	0.082	Cu	0.011	0.001
Mg	0.342	0.056	Cr	0.014	0.002
Si	0.646	0.046	Zn	0.072	0.004
Al	0.152	0.135	Mn	0.002	0.000
Cl	1.867	0.400	Sn	0.002	0.000
Br	0.070	0.002	Pb	0.006	0.000
Sb	0.114	0.021	Na	0.107	0.021
Ti	0.571	0.065	K	0.035	0.003
P	0.390	0.041	Sr	0.009	0.002

*The calculated error is based on three replicates

The recorded concentration of total bromine (Br; 0.070 ± 0.002 wt.%) along with that of the other regulated elements such as lead (Pb; 0.006 wt.%) and chromium (Cr; 0.014 ± 0.002 wt.%), complies with RoHS (Restriction of Hazardous Substances) regulation, hence allowing the recovery of the studied batch by means of mechanical recycling. Once again, the very small standard deviation reflects the reliability of the sampling method. It is worth mentioning that BFR-containing plastics were separated from the studied batch using an on-line X-ray detection as defined in the directive 2019/1021/EU (2019/1021/EU, 2019).

Br, antimony (Sb) and phosphorus (P) indicate the presence of flame retardants (FR) in the studied batch. Sb, in the form of antimony trioxide (Sb_2O_3), is used as a synergic agent of BFR thereby enhancing the bromine release from BFR by forming Sb_2Br_3 (Grause et al., 2010). Additionally, P-based FR such as phosphates, phosphites and melamine phosphates have been widely used in the last decades as value-added FR systems.

The small concentration of Zn (zinc) and Cr elements in the batch can be attributed to Ziegler-Natta and Philips catalysts used for polymerization process of PP and PE (Bichinho et al., 2005). Similarly, residual sodium persulfate ($Na_2S_2O_8$), a water-soluble initiator, used in the emulsion polymerization processes (Kumar and Gupta, 2003), can explain the presence of sodium (Na) and sulfur (S). Sulphites, are another S-based molecule commonly found in plastic parts because of their hydroperoxide inhibition properties.

The low Ti content (~0.57 ± 0.07 wt.%), originated from titanium dioxide (TiO_2), is related to the fact that unsortable WEEE streams are mainly constituted of dark colored plastic fractions, whereas TiO_2 is usually used as white pigment in PC/ABS blends (Taurino *et al.*, 2010).

Iron (Fe), nickel (Ni), and copper (Cu) XRF signals, can be explained by the presence of residual metallic parts that have not been removed during the sorting steps. Furthermore, the Fe-based barium ferrite ($BaFe_{12}O_{19}$) is frequently found in electrical equipment operating at microwave/GHz frequencies due to its electrical properties (Pullar, 2012).

The screening of the 500 Kg batch gives an interesting insight into the composition of a real unsortable post-consumer WEEE streams. The characterization of either bulk samples (~20 mm size) or batch representative samples has allowed a reliable quantification of the main polymers used in the manufacture of small EEE devices; styrene-based polymers (e.g. ABS, PS and HIPS), PP and PC account for more than 70% of the total organic components. The heterogeneity and complexity of the stream arise also from the detected inorganic/organic additives frequently used in the plastics industry. This phase accounts for 8 wt. % and includes calcium carbonate, mineral fillers, and fiberglass. More importantly, the recorded concentration of the RoHS restricted substances enables for mechanical recycling.

3.2. Relevance of EB irradiation to mechanical properties of unsortable WEEE plastics

391 Given the complex composition of the studied batch, electron beam (EB) irradiation was
392 considered as a means of compatibilization between the batch components. Indeed,
393 processing a complex polymer blend may give rise to materials with poor mechanical
394 properties as a consequence of polymers incompatibility and heterogeneity (Maris *et al.*,
395 2018). Irradiation of a complex polymer blend results in *in-situ* cross-linking reactions at the
396 interface leading to polymer compatibilization (Sonnier *et al.*, 2012). From a potential
397 industrial application perspective, EB-based ionizing radiation was adopted. Indeed, EB
398 technology is already used on an industrial scale for commercial purposes, does not generate
399 nuclear waste, is characterized by its short processing time and complies with restrictions on
400 volatile organic compounds emission (International Irradiation Association, 2011).

401 In the present work, two experimental pathways were investigated; the first one has
402 involved EB irradiation of micro-ground sample (< 500 µm particle size) prior to tween-screw
403 extrusion step, hereafter denoted as irradiated powder, while the second one has dealt with
404 irradiated extruded pellets, hereafter denoted as irradiated pellets. Non-irradiated pellets,
405 extruded irradiated powder and irradiated pellets were then injection molded and
406 mechanically characterized. Fig. 5 illustrates tensile strength and impact toughness results on
407 irradiated unsortable WEEE samples as a function of irradiation dose and experimental
408 procedure. The applied irradiation on powder has not a significant effect on the mentioned
409 properties. Except for elastic moduli (Fig. 5a), the mechanical behavior of the investigated
410 samples highlights irradiation dose and process dependency; stress at yield (Fig. 5b) of
411 irradiated pellets decreases after irradiation, while the EB irradiation undertaken on powder
412 does not show a significant evolution of the mentioned property. Additionally, the irradiation
413 dose is with no noteworthy impact on the irradiated powder elongation at break (Fig. 5c)
414 compared to that on the irradiated pellets, where a drop of the elongation at break was
415 observed. Regarding the impact toughness (Fig. 5d), the EB irradiation led to a slight decrease

of the sample toughness median value regardless of the applied irradiation dose and the experimental procedure. Nevertheless the wide range of the boxplot limits (i.e. Min-Max) of non-irradiated material highlights the material heterogeneity that probably hides the real effect of EB irradiation.

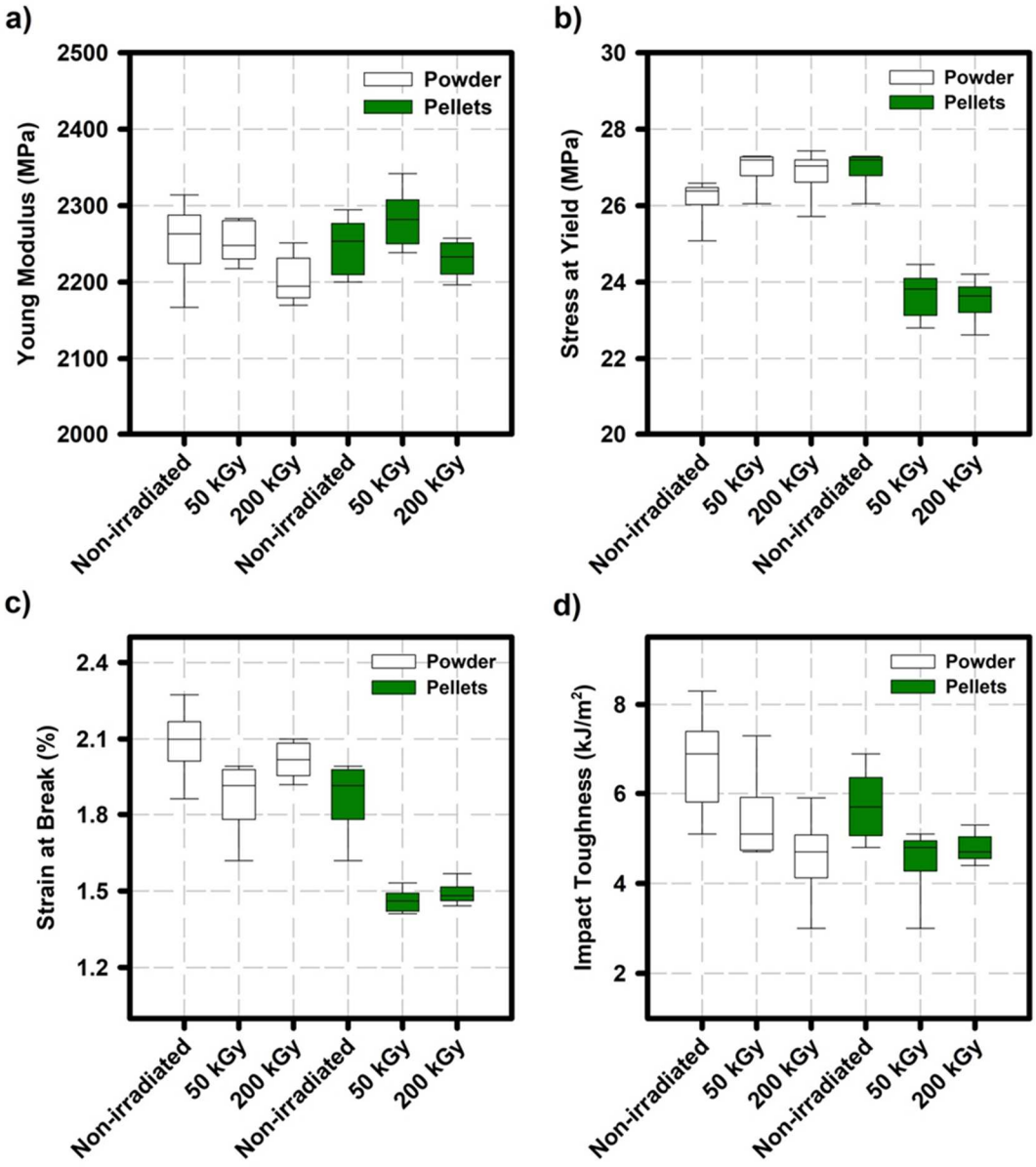

Fig. 5. a) Young modulus, b) stress at yield, c) strain at break and d) impact toughness for irradiated unsortable WEEE samples as a function of irradiation dose and experimental procedure (dog-bone specimens from irradiated powder or from irradiated pellets).

Based on these findings, it can be assumed that EB irradiation process does not really increase the adhesion through *in-situ* crosslinking and compatibilization between the different component phases of the investigated batch. Moreover, the decrease of elongation at break and impact toughness of the irradiated samples may result from a potential polymer chain degradation. In order to give more insight into this hypothesis, DSC analysis was carried out on injection molded bar specimens used for mechanical testing. The recorded DSC thermograms are displayed in Fig. 6. First, the heating DSC thermograms (Fig. 6a) of non-irradiated bars exhibit phase transitions similar to those for representative samples (Fig. 4a); two distinctive endothermic melting peaks around ~127 °C (T_m PE) and ~164 °C (T_m PP), as well as a styrene-based polymers glass transition at ~99 °C. On the contrary, the crystallization of PE component occurs at a delayed temperature (~131 °C), closer to that of PP, for non-irradiated processed sample (Fig. 6b), than for non-processed representative sample (Fig. S2). These observations might be indicative of PE dissolution in PP matrix in the molten state (Blom et *al.*, 1998). Besides, EB irradiation, particularly at 200 kGy, leads PP melting point to shift meaningfully to a lower temperature (T_m PP = ~154 °C) and PE melt enthalpy to decrease significantly (0.48 J/g for 200 kGy irradiated sample *vs.* 0.83 J/g for non-irradiated sample). In addition, the EB irradiation process gives rise to a single slightly shifted exothermic peak (Fig. 6b), representative of simultaneous crystallization of PP and PE, whereas it shows no impact on T_g of the styrenic polymers. It should be noted that DSC analysis on bar samples injection molded from irradiated pellets (Fig. S3) exhibits a similar trend to that presented in Fig. 6 with a PE crystallization occurring later than that of PP resulting in a broader PP melt peak.

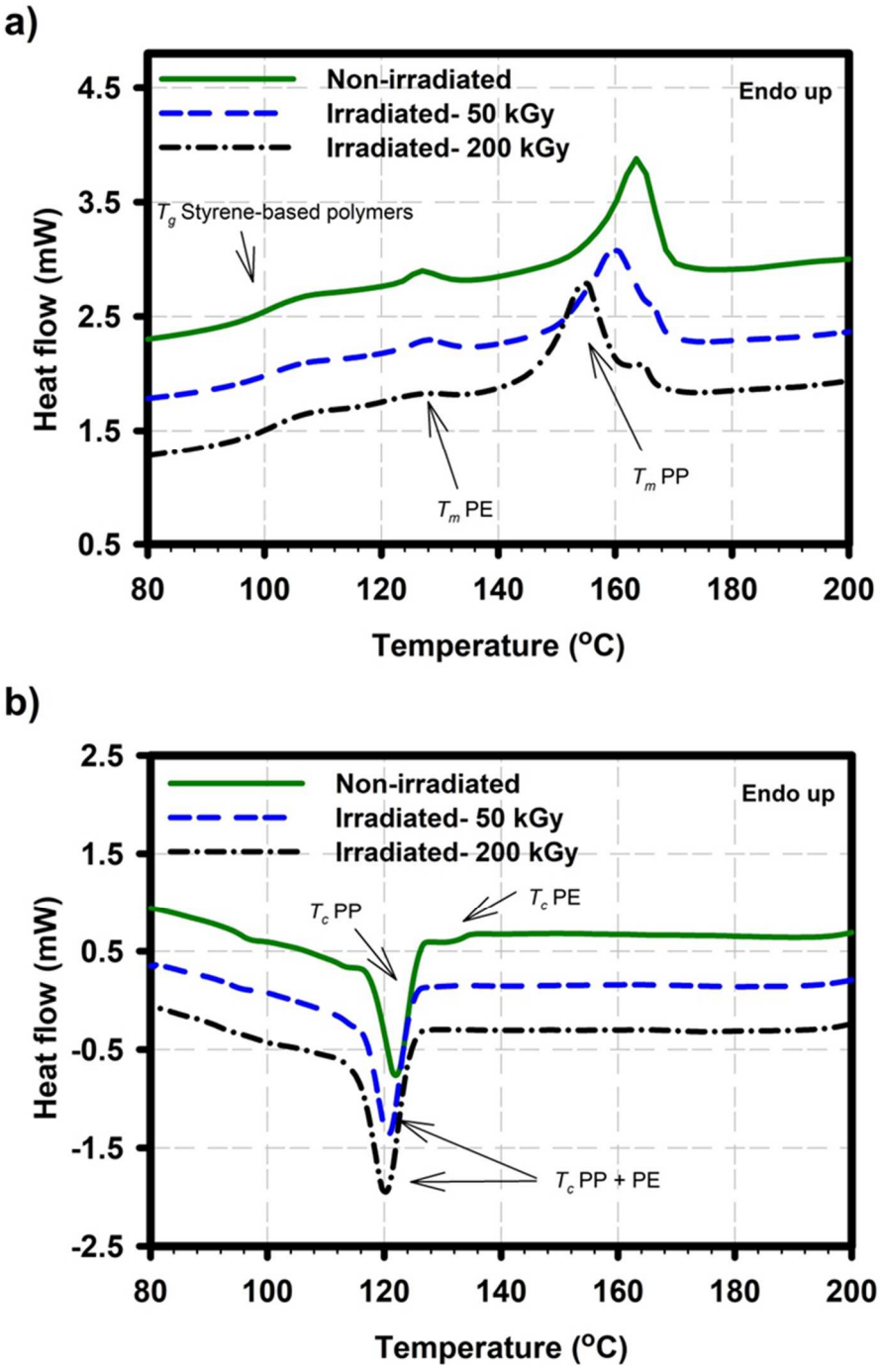

Fig. 6. DSC thermograms for bar specimens injection molded from irradiated then extruded powder at different irradiation dose (0, 50 and 200 kGy). a) 2nd heating cycle, and b) cooling cycle.

It has been demonstrated for PE/PP blends that the depression of both melting temperature and crystallinity rate indicates the miscibility phenomena (Li *et al.*, 2001), and that potential chemical interactions between macroradicals of irradiated PP and PE are favorable during

455 melt processing (Fel *et al.*, 2016). However, it is worth pointing out that melt temperature
456 decrease is also indicative of degraded polymers, and that crystallinity rate drop may be due
457 to their crosslinking. Given the complex composition of the studied batch, DSC was not able
458 to estimate the impact of irradiation on the other batch polymer components, that would have
459 provided supporting explanations for the observed mechanical behavior of irradiated samples.

460 Other methods such as electron paramagnetic resonance (EPR) and l,l-diphenyl-2-
461 picrylhydrazyl (DPPH) (unpublished results) failed to detect the persistence of macroradicals
462 in irradiated samples. Several key assumptions can be made: (1) EPR spectra are difficult to
463 interpret because of the complex batch composition; (2) The presence of Fe-based molecules
464 gives rise to anisotropic EPR spectra as the sample position changes; (3) The remaining
465 pigments in the batch hinder UV-absorbance of DPPH$^{\bullet}$ radicals; (4) Residual antioxidants and
466 free radical scavengers react with DPPH$^{\bullet}$ radicals.

467 Based on all the observations and discussion in this section, it can be hypothesized that upon
468 irradiation, PP undergoes β-chain scissions followed by crosslinking reactions with irradiated-
469 PE during melt processing stages, which may explain the decrease in the elongation at break
470 and impact toughness. On the other hand, although the irradiation may have led to free radical
471 production, the subsequent *in-situ* crosslinking reactions were not efficient enough to allow
472 compatibilization between the different polymer phases, and consequent mechanical
473 performance improvement of the final material. This can be explained by the complex
474 composition of the unsortable post-consumer WEEE stream and the presence of residual free
475 radical scavengers.

476

477 **4. Conclusions**

Mechanical recycling of plastics derived from post-consumer WEEE is an important waste management strategy. However, ~40% of this waste stream, named unsortable, are rejected from the classical NIR sorting lines as they don't comply with the sorted plastic streams and also because of their dark color. For the first time, a comprehensive examination of a real unsortable WEEE fraction has been investigated in the present work. The screening of the studied batch composition, based on FTIR analysis of 100 plastic parts (~ 20 mm size) and physico-chemical characterization of representative samples, allowed a reliable quantification and identification of different polymer types; including mainly ~50 % styrenic polymers, ~15 % PP, and ~15 % PC, and showed the existence of ~8 wt. % inorganic phase (calcium carbonate, talc and fiberglass). Most importantly, the concentration of total bromine, lead and chromium, in agreement with RoHS (Restriction of Hazardous Substances) regulation, gives evidence for the batch mechanical recycling.

Given the heterogenous composition of the 500 kg batch under investigation, EB irradiation, as a means of compatibilization between the batch components, was investigated. The potential recycling of the studied batch was evaluated through mechanical properties as function of irradiation dose (50 and 200 kGy) and experimental procedure (irradiated powder and irradiated pellets). Unlike irradiated powder, a significant drop of the elongation at break and stress at yield was detected for irradiated pellets regardless of the applied dose. Nevertheless, the impact toughness property was found to decrease independently of the applied irradiation dose and the experimental procedure. DSC analysis have shown potential PP β-chain scissions followed by crosslinking reactions with irradiated-PE during melt processing stages. This study has provided evidence that the behavior difference between a EB-irradiated unsortable post-consumer WEEE stream and a EB-irradiated virgin polymers blend, reported in the literature, is due to the complex composition of the stream and the presence of residual free radical scavengers which hinder *in-situ* crosslinking reactions

leading to the compatibilization between the different polymer phases. The present study shows that mechanical recycling simulation based on virgin polymer blend or sorted polymer waste is not representative of real post-consumer unsortable streams. This work may spur further studies on other ways of compatibilization in order to improve mechanical properties and cost-effectiveness.

Author contributions section

Imane Belyamani: Conceptualization, Methodology, Validation, Formal analysis, Investigation, Data Curation, Supervision, Writing-original Draft, Writing- Review and Editing, Visualization. **Joachim Maris**: Conceptualization, Methodology, Validation, Formal analysis, Investigation, Data Curation. **Sylvie Bourdon**: Conceptualization, Supervision, Writing- Review and Editing, resources, funding acquisition. **Jean-Michel Brossard**: Conceptualization, Validation, Supervision, Writing- Review and Editing, resources, funding acquisition. **Laurent Cauret**: Conceptualization, Methodology, Validation, Supervision. **Laurent Fontaine**: Conceptualization, Methodology, Validation, supervision. **Véronique Montembault**: Conceptualization, Methodology, Validation, Project administration, Supervision, Writing- Review and Editing.

Acknowledgments.

We acknowledge financial support from Veolia Research & Innovation and ANRT (Association National de la Recherche et de la Technologie).

Additional Supporting Information may be found in the online version of this article.

527 **References**

528 2012/19/EU, 2012. Directive 2012/19/EU of the European Parliament and of the Council of 4
529 July 2012 on waste electrical and electronic equipment.
530 2019/1021/EU, 2019. Regulation (EU) 2019/1021 of the European Parliament and of the
531 Council - of 20 June 2019 - on persistent organic pollutants.
532 Afnor, 2018. XP CEN/TS 17188 standard: Prélèvement et échantillonnage de granulats.
533 Alwaeli, M., 2011. Economic calculus of the effectiveness of waste utilization processed as
534 substitutes of primary materials. Environ. Prot. Eng. 37, 51-58.
535 Bao, Y., Zhi-ming, H., Shen-xing, L., Zhi-xue, W., 2008. Thermal stability, smoke emission
536 and mechanical properties of poly (vinyl chloride)/hydrotalcite nanocomposites.
537 Polym. Degrad. Stab. 93, 448–455.
538 https://doi.org/10.1016/j.polymdegradstab.2007.11.014
539 Bichinho, K.M., Pires, G.P., Stedile, F.C., Santos, J.H.Z. dos, Wolf, C.R., 2005.
540 Determination of catalyst metal residues in polymers by X-ray fluorescence.
541 Spectrochim. Acta Part B At. Spectrosc. 60, 599–604.
542 https://doi.org/10.1016/j.sab.2004.11.012
543 Blom, H.P., Teh, J.W., Bremner, T., Rudin, A., 1998. Isothermal and non-isothermal
544 crystallization of PP: effect of annealing and of the addition of HDPE. Polymer 39,
545 4011–4022. https://doi.org/10.1016/S0032-3861(97)10305-6
546 Bovea, M.D., Pérez-Belis, V., Ibáñez-Forés, V., Quemades-Beltrán, P., 2016. Disassembly
547 properties and material characterisation of household small waste electric and
548 electronic equipment. Waste Manag. 53, 225–236.
549 https://doi.org/10.1016/j.wasman.2016.04.011
550 Burillo, G., Clough, R.L., Czvikovszky, T., Guven, O., Le Moel, A., Liu, W., Singh, A.,
551 Yang, J., Zaharescu, T., 2002. Polymer recycling: potential application of radiation

552 technology. Radiat. Phys. Chem. 64, 41–51. https://doi.org/10.1016/S0969-
553 806X(01)00443-1
554 Chancerel, P., Rotter, S., 2009. Recycling-oriented characterization of small waste electrical
555 and electronic equipment. Waste Manag. 29, 2336–2352.
556 https://doi.org/10.1016/j.wasman.2009.04.003
557 Chmielewski, A.G., Haji-Saeid, M., Ahmed, S., 2005. Progress in radiation processing of
558 polymers. Nucl. Instrum. Methods Phys. Res. Sect. B Beam Interact. Mater. At.,
559 Ionizing Radiation & Polymers 236, 44–54.
560 https://doi.org/10.1016/j.nimb.2005.03.247
561 Czégény, Z., Jakab, E., Blazsó, M., Bhaskar, T., Sakata, Y., 2012. Thermal decomposition of
562 polymer mixtures of PVC, PET and ABS containing brominated flame retardant:
563 Formation of chlorinated and brominated organic compounds. J. Anal. Appl. Pyrolysis
564 96, 69–77. https://doi.org/10.1016/j.jaap.2012.03.006
565 Dimitrakakis, E., Janz, A., Bilitewski, B., Gidarakos, E., 2009. Small WEEE: Determining
566 recyclables and hazardous substances in plastics. J. Hazard. Mater. 161, 913–919.
567 https://doi.org/10.1016/j.jhazmat.2008.04.054
568 Dolores, A. J., Lasco, J. D. D., Bertiz, T. M., Lamar, K. M. 2020. Compressive Strength and
569 Bulk Density of Concrete Hollow Blocks (CHB) Infused with Low-Density
570 Polyethylene (LDPE) Pellets. 6, 1932-1943. http://dx.doi.org/10.28991/cej-2020-
571 03091593
572 Drobny, J.G., 2010. Radiation technology for polymers. CRC press.
573 Epsztein, S.R., de Fombelle, M.A.J., Falher, T., Jouannet, D., Gallone, T., Cauret, L., 2014.
574 Substitution of Virgin material by recycled material from End-of-Life Vehicle (ELV).
575 Presented at the Key Engineering Materials, Trans Tech Publ, pp. 836–843.
576 https://doi.org/10.4028/www.scientific.net/KEM.611-612.836

577 Fel, E., Khrouz, L., Massardier, V., Cassagnau, P., Bonneviot, L., 2016. Comparative study of
578 gamma-irradiated PP and PE polyolefins part 2: Properties of PP/PE blends obtained
579 by reactive processing with radicals obtained by high shear or gamma-irradiation.
580 Polymer 82, 217–227. https://doi.org/10.1016/j.polymer.2015.10.070
581 Gardette, J.-L., Mailhot, B., Lemaire, J., 1995. Photooxidation mechanisms of styrenic
582 polymers. Polym. Degrad. Stab. 48, 457–470. https://doi.org/10.1016/0141-
583 3910(95)00113-Z
584 Ghorbel, E., Hadriche, I., Casalino, G., Masmoudi, N., 2014. Characterization of thermo-
585 mechanical and fracture behaviors of thermoplastic polymers. Materials 7, 375–398.
586 https://doi.org/10.3390/ma7010375
587 Gramatyka, P., Nowosielski, R., Sakiewicz, P., 2007. Recycling of waste electrical and
588 electronic equipment. J. Achiev. Mater. Manuf. Eng. 20, 535–538.
589 https://doi.org/10.12691/ajmr-6-1-3
590 Grause, G., Ishibashi, J., Kameda, T., Bhaskar, T., Yoshioka, T., 2010. Kinetic studies of the
591 decomposition of flame retardant containing high-impact polystyrene. Polym. Degrad.
592 Stab. 95, 1129–1137. https://doi.org/10.1016/j.polymdegradstab.2010.02.008
593 Gu, J., Xu, H., Wu, C., 2014. Thermal and Crystallization Properties of HDPE and HDPE/PP
594 Blends Modified with DCP. Adv. Polym. Technol. 33.
595 https://doi.org/10.1002/adv.21384
596 Gy, P., 1998. Sampling for analytical purposes. John Wiley & Sons.
597 Hamaide, T., Deterre, R., Feller, J.-F., 2014. Environmental impact of polymers. John Wiley
598 & Sons.
599 Hennebert, P., 2017. WEEE plastic sorting for bromine content is essential to enforce EU
600 regulation.

Huy, T.A., Adhikari, R., Lüpke, T., Henning, S., Michler, G.H., 2004. Molecular deformation mechanisms of isotactic polypropylene in α-and β-crystal forms by FTIR spectroscopy. J. Polym. Sci. Part B Polym. Phys. 42, 4478–4488. https://doi.org/10.1002/polb.20117

International Irradiation Association, 2011. Industrial Radiation with Electron Beams and X-rays.

Ismail, H., Hanafiah, M.M., 2019. An overview of LCA application in WEEE management: Current practices, progress and challenges. J. Clean. Prod. 232, 79–93. https://doi.org/10.1016/j.jclepro.2019.05.329

Kang, H.-Y., Schoenung, J.M., 2005. Electronic waste recycling: A review of U.S. infrastructure and technology options. Resour. Conserv. Recycl. 45, 368–400. https://doi.org/10.1016/j.resconrec.2005.06.001

Karahaliou, E., Tarantili, P., 2009. Stability of ABS compounds subjected to repeated cycles of extrusion processing. Polym. Eng. Sci. 49, 2269–2275. https://doi.org/10.1002/pen.21480

Kumar, A., Gupta, R.K., 2003. Fundamentals of Polymer Engineering. Marcel Dekker, Inc, New York.

Kyere, V.N., Greve, K., Atiemo, S. M., Amoako, D., Kwame Aboh, I.J., Cheabu, B. 2018. Contamination and Health risk Assessment of Exposure to Heavy Metals in Soils from Informal E-Waste Recycling Site in Ghana. Emerg. Sci. J. 2, 428-436. http://dx.doi.org/10.28991/esj-2018-01162Lacoste, J., Delor, F., Pilichowski, J., Singh, R., Prasad, A.V., Sivaram, S., 1996. Polybutadiene content and microstructure in high impact polystyrene. J. Appl. Polym. Sci. 59, 953–959. https://doi.org/10.1002/(SICI)1097-4628(19960207)59:6<953::AID-APP7>3.0.CO;2-O

626 Lambla, M., Seadan, M., 1993. Reactive blending of polymers by interfacial free-radical
627 grafting. Makromol. Chem. Macromol. Symp. 69, 99–123.
628 https://doi.org/10.1002/masy.19930690112
629 Lambla, M., Seadan, M., 1992. Interfacial grafting and crosslinking by free radical reactions
630 in polymer blends. Polym. Eng. Sci. 32, 1687–1694.
631 https://doi.org/10.1002/pen.760322206
632 Li, J., Li, C., Liao, Q., Xu, Z., 2019. Environmentally-friendly technology for rapid on-line
633 recycling of acrylonitrile-butadiene-styrene, polystyrene and polypropylene using
634 near-infrared spectroscopy. J. Clean. Prod. 213, 838–844.
635 https://doi.org/10.1016/j.jclepro.2018.12.160
636 Li, J., Shanks, R.A., Olley, R.H., Greenway, G.R., 2001. Miscibility and isothermal
637 crystallisation of polypropylene in polyethylene melts. Polymer 42, 7685–7694.
638 https://doi.org/10.1016/S0032-3861(01)00248-8
639 Li, R., Zhang, X., Zhou, L., Dong, J., Wang, D., 2009. In situ compatibilization of
640 polypropylene/polystyrene blend by controlled degradation and reactive extrusion. J.
641 Appl. Polym. Sci. 111, 826–832. https://doi.org/10.1002/app.29118
642 Li, Y., Wu, X., Song, J., Li, J., Shao, Q., Cao, N., Lu, N., Guo, Z., 2017. Reparation of
643 recycled acrylonitrile-butadiene-styrene by pyromellitic dianhydride: reparation
644 performance evaluation and property analysis. Polymer 124, 41–47.
645 http://dx.doi.org/10.1016/j.polymer.2017.07.042
646 Liang, C.Y., Krimm, S., 1958. Infrared spectra of high polymers. VI. Polystyrene. J. Polym.
647 Sci. 27, 241–254. https://doi.org/10.1002/pol.1958.1202711520
648 Maris, E., Botané, P., Wavrer, P., Froelich, D., 2015. Characterizing plastics originating from
649 WEEE: A case study in France. Miner. Eng., Sustainable Minerals 76, 28–37.
650 https://doi.org/10.1016/j.mineng.2014.12.034

651 Maris, J., Bourdon, S., Brossard, J.-M., Cauret, L., Fontaine, L., Montembault, V., 2018.
652 Mechanical recycling: Compatibilization of mixed thermoplastic wastes. Polym.
653 Degrad. Stab. 147, 245–266. https://doi.org/10.1016/j.polymdegradstab.2017.11.001
654 Martinho, G., Pires, A., Saraiva, L., Ribeiro, R., 2012. Composition of plastics from waste
655 electrical and electronic equipment (WEEE) by direct sampling. Waste Manag. 32,
656 1213–1217. https://doi.org/10.1016/j.wasman.2012.02.010
657 McNeill, I.C., Memetea, L., Cole, W.J., 1995. A study of the products of PVC thermal
658 degradation. Polym. Degrad. Stab. 49, 181–191. https://doi.org/10.1016/0141-
659 3910(95)00064-S
660 Menad, N.-E., 2016. Chapter 3 - Physical Separation Processes in Waste Electrical and
661 Electronic Equipment Recycling, in: Chagnes, A., Cote, G., Ekberg, C., Nilsson, M.,
662 Retegan, T. (Eds.), WEEE Recycling. Elsevier, pp. 53–74.
663 https://doi.org/10.1016/B978-0-12-803363-0.00003-1
664 Milad, A., Ali, A. S. B., Yusoff, N. I. M. 2020. A Review of the Utilisation of Recycled
665 Waste Material as an alternative Modifier in Asphalt Mixtures. J. Civ. Eng. 6, 42-60.
666 http://dx.doi.org/10.28991/cej-2020-SP(EMCE)-05
667 Munteanu, S., Vasile, C., 2005. Spectral and thermal characterization of styrene-butadiene
668 copolymers with different architectures. J. Optoelectron. Adv. Mater. 7, 3135.
669 Numata, S., Fujii, Y., 1995. Improved flexural properties of polymer blends by mixing with a
670 multifunctional monomer and crosslinking with gamma-rays. Plast. Rubber Compos.
671 Process. Appl 5, 293–300.
672 Parajuly, K., Wenzel, H., 2017. Potential for circular economy in household WEEE
673 management. J. Clean. Prod. 151, 272–285.
674 https://doi.org/10.1016/j.jclepro.2017.03.045

675 Pullar, R.C., 2012. Hexagonal ferrites: A review of the synthesis, properties and applications
676 of hexaferrite ceramics. Prog. Mater. Sci. 57, 1191–1334.
677 https://doi.org/10.1016/j.pmatsci.2012.04.001
678 Sahajwalla, V., Gaikwad, V., 2018. The present and future of e-waste plastics recycling. Curr.
679 Opin. Green Sustain. Chem., Reuse and Recycling / UN SGDs: How can Sustainable
680 Chemistry Contribute? / Green Chemistry in Education 13, 102–107.
681 https://doi.org/10.1016/j.cogsc.2018.06.006
682 Said, H.M., Khafaga, M.R., El-Naggar, A.W.M., 2013. Compatibilization of Poly (ethylene
683 terephthalate)/Low Density Polyethylene Blends by Gamma Irradiation and Graft
684 Copolymers. Arab J. Nucl. Sci. Appl. 46, 56–69.
685 Satapathy, S., Chattopadhyay, S., Chakrabarty, K.K., Nag, A., Tiwari, K.N., Tikku, V.K.,
686 Nando, G.B., 2006. Studies on the effect of electron beam irradiation on waste
687 polyethylene and its blends with virgin polyethylene. J. Appl. Polym. Sci. 101, 715–
688 726. https://doi.org/10.1002/app.23970
689 Silas, R.S., Yates, J., Thornton, V., 1959. Determination of unsaturation distribution in
690 polybutadienes by infrared spectrometry. Anal. Chem. 31, 529–532.
691 https://doi.org/10.1021/ac50164a022
692 Sonnier, R., Taguet, A., Rouif, S., 2012. Modification of polymer blends by E-beam and
693 Gamma-irradiation, in: Functional Polymer Blends: Synthesis, Properties, and
694 Performance. Boca Raton CRC Press, pp. 261–304.
695 Stenvall, E., Tostar, S., Boldizar, A., Foreman, M.R.S., Möller, K., 2013. An analysis of the
696 composition and metal contamination of plastics from waste electrical and electronic
697 equipment (WEEE). Waste Manag. 33, 915–922.
698 https://doi.org/10.1016/j.wasman.2012.12.022

699 Stockholm Convention, 2017. Guidance on best available techniques and best environmental
700 practices for the recycling and disposal of wastes containing polybrominated diphenyl
701 ethers (PBDEs) listed under the Stockholm Convention on Persistent Organic
702 Pollutants. Stockholm Convention.
703 Taurino, R., Pozzi, P., Zanasi, T., 2010. Facile characterization of polymer fractions from
704 waste electrical and electronic equipment (WEEE) for mechanical recycling. Waste
705 Manag. 30, 2601–2607. 10.1016/j.wasman.2010.07.014
706 Tostar, S., Stenvall, E., Foreman, M., Boldizar, A., 2016. The Influence of Compatibilizer
707 Addition and Gamma Irradiation on Mechanical and Rheological Properties of a
708 Recycled WEEE Plastics Blend. Recycling 1, 101–110.
709 .https://doi.org/10.3390/recycling1010101
710 Utracki, L.A., 2002. Compatibilization of Polymer Blends. Can. J. Chem. Eng. 80, 1008–
711 1016. https://doi.org/10.1002/cjce.5450800601
712 Vazquez, Y.V., Barbosa, S.E., 2016. Recycling of mixed plastic waste from electrical and
713 electronic equipment. Added value by compatibilization. Waste Manag. 53, 196–203.
714 https://doi.org/10.1016/j.wasman.2016.04.022
715 Vilaplana, F., Ribes-Greus, A., Karlsson, S., 2006. Degradation of recycled high-impact
716 polystyrene. Simulation by reprocessing and thermo-oxidation. Polym. Degrad. Stab.
717 91, 2163–2170. 10.1016/j.polymdegradstab.2006.01.007
718 Vivier, T., Xanthos, M., 1994. Peroxide modification of a multicomponent polymer blend
719 with potential applications in recycling. J. Appl. Polym. Sci. 54, 569–575.
720 https://doi.org/10.1002/app.1994.070540507
721 Wang, R., Xu, Z., 2014. Recycling of non-metallic fractions from waste electrical and
722 electronic equipment (WEEE): A review. Waste Manag. 34, 1455–1469.
723 https://doi.org/10.1016/j.wasman.2014.03.004

724 Widmer, R., Oswald-Krapf, H., Sinha-Khetriwal, D., Schnellmann, M., Böni, H., 2005.
725 Global perspectives on e-waste. Environ. Impact Assess. Rev., Environmental and
726 Social Impacts of Electronic Waste Recycling 25, 436–458.
727 https://doi.org/10.1016/j.eiar.2005.04.001
728 Xanthos, M., Dagli, S.S., 1991. Compatibilization of polymer blends by reactive processing.
729 Polym. Eng. Sci. 31, 929–935. https://doi.org/10.1002/pen.760311302
730 Zhu, Z., Kelley, M.J., 2005. IR spectroscopic investigation of the effect of deep UV
731 irradiation on PET films. Polymer 46, 8883–8891.
732 https://doi.org/10.1016/j.polymer.2005.05.135
733